

GRAPHICAL POSTERIOR PREDICTIVE CLASSIFIER: BAYESIAN MODEL AVERAGING WITH PARTICLE GIBBS

TATJANA PAVLENKO AND FELIX LEOPOLDO RIOS

ABSTRACT. In this study, we present a multi-class graphical Bayesian predictive classifier that incorporates the uncertainty in the model selection into the standard Bayesian formalism. For each class, the dependence structure underlying the observed features is represented by a set of decomposable Gaussian graphical models. Emphasis is then placed on the *Bayesian model averaging* which takes full account of the class-specific model uncertainty by averaging over the posterior graph model probabilities. Even though the decomposability assumption severely reduces the model space, the size of the class of decomposable models is still immense, rendering the explicit Bayesian averaging over *all* the models infeasible. To address this issue, we consider the particle Gibbs strategy of Olsson et al. (2016) for posterior sampling from decomposable graphical models which utilizes the Christmas tree algorithm of Rios et al. (2016) as proposal kernel. We also derive the a strong hyper Markov law which we call the *hyper normal Wishart law* that allow to perform the resultant Bayesian calculations locally. The proposed predictive graphical classifier reveals superior performance compared to the ordinary Bayesian predictive rule that does not account for the model uncertainty, as well as to a number of out-of-the-box classifiers.

1. INTRODUCTION

A Bayesian supervised predictive classifier is presented for a multi-class classification problem where class distributions are represented by graphical models. The goal is to decide a class-membership of a new observation, and assess the uncertainty related to the decision rule conditional on all relevant information available.

Suppose that a set $\mathbf{n} = \{1, \dots, n\}$ of data items is given where each item belongs to one of k source classes denoted by Π_1, \dots, Π_k . Working in a supervised setting, we further assume that all the eligible classes are a priori specified. We introduce a discrete random variable, \mathcal{C} , with $\mathcal{C} = c$ denoting membership of Π_c , $c = 1, \dots, k$ and assume the class labels to be known for all the samples in \mathbf{n} .

Our Bayesian approach calls for a prior on \mathcal{C} , and we will assume that this prior, represented by the probability mass function $p_{\mathcal{C}}(c)$, $\sum_{c \in \mathcal{C}} p_{\mathcal{C}}(c) = 1$, is also known. With $p_{\mathcal{C}}(c)$ unknown, by treating \mathcal{C} as a multinomial random variable, we can use the family of Dirichlet priors to obtain the posterior probabilities over an ensemble of classes.

Associated with each item is a vector $\mathbf{x} = (x_1, \dots, x_p)'$, a collection of p continuous feature variables. Each such vector assigned to a particular class Π_c is assumed to be generated from a class-specific distributions with the density $f(\mathbf{x} | \theta_c)$ with $\theta_c \in \Theta_c$, where Θ_c is the associated parameter space. Suppose further that we have observed the values of

\mathcal{C} and all the \mathbf{x} 's for a random sample of n items, yielding the *training data*

$$\{(\mathcal{C}_i, \mathbf{x}^i)\}_{i=1}^n, \quad n = n_1 + \cdots + n_k.$$

Let \mathbf{C}^n denote the the vector $(\mathcal{C}_1, \dots, \mathcal{C}_n)$, and $\mathbf{x}^{(n)}$ be the sample vectors for items in the training data. For any subset $\mathbf{a} \subset \mathbf{n}$, we use $\mathbf{x}^{(a)} \subset \mathbf{x}^{(n)}$ to denote the subsets of data for the corresponding samples. In what follows, we generally use the upper indices to denote sample observations and save lower indices for structural properties of the observed \mathbf{x} .

Suppose further that we are presented with a "future" [or "fresh" or new "test"] observation, an item given by a vector \mathbf{x}^{n+1} of observed features. Given the above set up, we are interested in making inference about the value of \mathcal{C}_{n+1} which is the main target of predictive inference, (i.e. decide class-membership) of the new observation on the basis of all the available data $(\mathbf{C}^n, \mathbf{x}^{(n)}, \mathbf{x}^{n+1})$. This problem of classification can be formulated as a process of determining posterior probabilities for Π_1, \dots, Π_k , i.e. posterior distribution of \mathcal{C}_{n+1} for all the classes.

$$(1) \quad p_{\mathcal{C}_{n+1}}(c \mid \mathbf{x}^{n+1}, \mathbf{x}^{(n_c)}, \mathbf{C}^n) = \frac{f(\mathbf{x}^{n+1} \mid c, \mathbf{x}^{(n_c)}, \mathbf{C}^n) p_{\mathcal{C}_{n+1}}(c \mid \mathbf{C}^n)}{\sum_{c' \in \{1, \dots, k\}} f(\mathbf{x}^{n+1} \mid c', \mathbf{x}^{(n_{c'})}, \mathbf{C}^n) p_{\mathcal{C}_{n+1}}(c' \mid \mathbf{C}^n)},$$

where

$$(2) \quad f(\mathbf{x}^{n+1} \mid \mathbf{x}^{(n_c)}, c, \mathbf{C}^n) = \int_{\Theta_c} f(\mathbf{x}^{n+1} \mid \theta_c) f(\theta_c \mid \mathbf{x}^{(n_c)}, \mathbf{C}^n) d\theta_c$$

is the predictive probability distribution of \mathbf{x}^{n+1} with the class Π_c , and

$$(3) \quad p_{\mathcal{C}_{n+1}}(c \mid \mathbf{C}^n) = \int p(c \mid \phi_c) f(\phi_c \mid \mathbf{C}^n) d\phi_c,$$

is the prior probability of the class c parameterized by ϕ_c .

Further, the optimal classification rule corresponding to zero-one loss function (assigning zero cost to any correct decision, and unit cost to any wrong decision) can be obtained by specifying the mode of the posterior distribution in (1). This is referred to as the *maximum a posteriori (MAP) criterion* that can be further simplified to

$$(4) \quad c^* = \arg \max_{c \in \{1, \dots, k\}} p(c \mid \mathbf{x}^{n+1}, \mathbf{x}^{(n)}, \mathbf{C}^n) = \arg \max_{c \in \{1, \dots, k\}} f(\mathbf{x}^{n+1} \mid c, \mathbf{x}^{(n)}, \mathbf{C}^n) p(c \mid \mathbf{C}^n),$$

yielding the Bayesian predictive classifier which assigns \mathbf{x}^{n+1} to Π_{c^*} . The classification rule that assigns a class membership of a new observation \mathbf{x}^{n+1} by using the the MAP estimator of $p_{\mathcal{C}_{n+1}}(c \mid \mathbf{x}^{n+1}, \mathbf{x}^{(n)}, \mathbf{C}^n)$, is known to be optimal in a sense that it minimizes the averaged risk of misclassification (see e.g. Ripley (2007)).

Foundations of the general predictive Bayesian inference, with the focus on the predictive classification are considered in pioneering works by Geisser, see Geisser (1964, 1966, 1993). Several such predictive classifiers have been later emerged in the literature and their performance properties have been studied. Examples include e.g. Dawid and Fang (1992) where the supervised Bayesian classification has been studied using natural conjugate priors for the Gaussian distribution parameters and with infinitely many feature variables. Class specific predictive distributions are derived in such growing dimensions

asymptotic framework along with the conditions that allows almost sure identification of the class membership of a sample from an unknown origin.

Further extensions of the posterior predictive strategy within classification framework are considered in the recent studies by Corander et al. (2013c), and Nyman et al. (2016) where the key component is the incorporation of the structural properties of the class-conditional distributions into the Bayesian predictive inference. These structural properties describe the qualitative manner in which information flows among the feature variables and are well-represented by a *graphical model*, $G = (V, E)$ where the nodes V , representing random variables in the model, are connected by undirected edges $E \subseteq V \times V$, encoding the conditional independence properties of the multivariate distribution Lauritzen (1996).

In Corander et al. (2013c), the class-specific distributions are represented by a family of Gaussian graphical models (GGMs) with the block-diagonal structure, which is then conveniently merged with the conjugate Bayesian analysis. Due to the factorization of the posterior predictive densities over the graph structure, such type of assumption allows for local, within-blocks Bayesian updates, which in turn delivers an efficient solution to the high-dimensional classification problems, see details in Corander et al. (2013c). Nyman et al. (2016) , consider classification of categorical data where the class of stratified decomposable graphical models is used for encoding feature dependencies. This approach is shown to allow for a more detailed representation of the dependence structure, thus enhancing the classification process.

The above mentioned classifiers, while usually called predictive, are in fact derived under a single *known* graph G defining the class-conditional distribution and hence do not generally obey the principles of the predictive Bayesian inference in the sense of Geisser (1993). Conditioning on G , while essentially simplifying the posterior analysis, ignores the uncertainty the model themselves possess on the probabilistic classification. We argue therefore that the standard predictive classification formalism stated in equations (1)-(3) is flawed and suggest a generic framework for the Bayesian treatment of model uncertainty. Specifically, for each Π_c , we consider the underlying class-specific graph, G_c as *unknown*, and characterize it through its posterior distribution which is in turn incorporated into the building of the predictive classifier.

Bayesian inference concerning the graph G is usually referred to a *structure learning* and requires specification of a flexible but tractable family \mathcal{G} of possible graphs, capable of representing a variety of the conditional independence structure. Although other types of graphical models exist, in the interests of tractability and scalability, we for each Π_c , restrict the family \mathcal{G} to the set of *undirected decomposable Gaussian graphical models*, and allow the graph structure freely vary across different classes within \mathcal{G} . The family \mathcal{G} exhibits the special property that for each $G \in \mathcal{G}$, the Markov distribution over G can be derived recursively, by using Markov combinations of smaller components, see details in Section 2. Prior distributions over the graphical structure itself, which are termed for *graph laws* are discussed in detail in Byrne and Dawid (2015).

The first key component of our suggested approach is the *Bayesian model averaging*, where the posterior predictive distribution of \mathbf{x}^{n+1} in (2) under each of the candidate models in \mathcal{G} is weighted by the posterior model probabilities. Theoretically, Madigan and Raftery

(1994) show that Bayesian averaging over *all* the models in this fashion provides better predictive accuracy than using any single model; see Dawid (1986) and Kass and Raftery (1995) for a review of general Bayesian model averaging approach and a more recent review on the evaluation of Bayesian approaches for model uncertainty by Clyde and George (2004). But even though the graph decomposability assumption severely reduces the model space, the size of the family of decomposable is still immense, rendering the explicit Bayesian averaging over all potential structures in \mathcal{G} infeasible. To tackle this issue, we exploit the *particle Markov chain Monte Carlo* (PMCMC) sampling strategy to obtain an approximation of the graph posterior distribution. This bring us to the second key component of our approach, namely *Particle Gibbs with systematic refreshments* (PG) sampling scheme which is designed for efficient posterior sampling from decomposable graphical models; see details in Olsson et al. (2016) and a companion paper Rios et al. (2016). Combined, the two components constitute our new, inherently predictive classification procedure, called for the *graphical posterior predictive* classifier. For a general review of particle MCMC methods, see e.g. Andrieu et al. (2010) and Chopin and Singh (2015).

In a series of papers, Corander et al. (2013a,b) and Cui et al. (2016) have addressed another important issue of the predictive inference in both supervised and semi-supervised settings, namely using *marginal* and *simultaneous* predictive classifiers. Simultaneous classifiers require modeling of the *joint* posterior predictive distribution of the unknown class variables for the test sample and are therefore computationally much more demanding than the standard, marginal ones which treat each fresh observation separately and independently on the other observations in the test data.

Performance properties of simultaneous and marginal supervised classifiers are extensively studied in Cui et al. (2016), indicating that both approaches demonstrate asymptotically equal performance accuracy when the amount of training data goes to infinity (Cui et al., 2016, Theorem 1, Theorem 2). In the light of results, we in the current study focus on the marginal predictive strategy, noting however that our proposed graphical predictive classifier is fully suitable for the simultaneous Bayesian inference.

The structure of the remaining part of the paper is as follows. In Section 2, we review the properties of the hyper Markov laws over decomposable GGMs (Dawid and Lauritzen (1993)), introduce the hyper normal inverse Wishart conjugate family of prior distributions and show that it is strong hyper Markov. Using these results, we then in Section 3 derive our graphical predictive classifier that is based on the predictive distribution (predictive score function) for \mathbf{x}^{n+1} and incorporates Bayesian model averaging over \mathcal{G} . In Section 4, we derive the MCMC graph structure learning algorithm which is needed for approximating the graph posterior at the model averaging step. This algorithm, recently suggested in Olsson et al. (2016) is based on the particle Gibbs graph structure learning that exploits the Christmas tree kernel presented in the companion paper Rios et al. (2016), and allows for an efficient posterior sampling form the decomposable GGMs. Next in Section 5, we provide the description and results of our numerical study. We conclude in Section 6 with some computational considerations and future research directions. Technical derivations are found in Appendix A.

2. REVIEW OF GRAPH THEORY AND MARKOV PROPERTIES

For consistency and clarity of the presentation, we restate some definitions and results regarding graph theory and Markov properties which will be used later in this text. For further details the reader is referred to Lauritzen (1996) and Dawid and Lauritzen (1993).

Let $G = (V, E)$ be an undirected graph with node set V and edge set $E \subseteq V \times V$. Two nodes $a, b \in V$ are said to be neighbors in G if $(a, b) \in E$. A subset $Q \subseteq V$ is complete if every pair of nodes $(a, b) \in E$ are neighbors in the subgraph G_Q , induced by the nodes in Q . If Q is maximal, in the sense that it is not contained in any other complete set of nodes it is called a clique.

Definition 1. *A decomposition of G is a pair (A, B) such that $A \cup B = V$, $A \cap B$ is complete and separates A from B , that is, every path between nodes in A and B must intersect $A \cap B$.*

Henceforth in this paper we will assume that G is *decomposable* defined next.

Definition 2. *A graph G is decomposable if it is complete or if there exists a decomposition (A, B) of G such that G_A and G_B are decomposable.*

Decomposable graphs are sometimes alternatively termed *chordal* or *triangulated*, as Definition 2 is equivalent to the requirement that every cycle of length 4 or more is chorded. Decomposable graphs are also characterized by the fact that their cliques can be arranged in a so called *junction tree*.

Theorem 3. *A graph G is decomposable if and only if its cliques can be arranged in a junction tree, meaning that for any pair of cliques Q_i, Q_j it holds that $Q_i \cap Q_j \subseteq Q$, for every clique Q on the unique path between Q_i and Q_j .*

The intersections of two neighboring cliques in a junction tree is called a *separator*. We denote the set of separators by \mathcal{S} and the set of cliques by \mathcal{Q} . Since the graph, G underlying a junction tree is unique, \mathcal{Q} and \mathcal{S} can also be regarded as components of G itself. The space of all decomposable graphs with a given number of nodes, which should be understood from the context, is denoted by \mathcal{G} . A junction tree for a specific graph G is not unique in general, following the notation in Thomas and Green (2009) we denote the number of equivalent junction trees by $\mu(G)$. On the other hand, each junction tree T has exactly one underlying decomposable graph which we denote by $g(T)$.

Let $X = (X_i)_{i \in V}$ be a random variable and let $f(\mathbf{x}_A)$ denote a generic marginal density function of $X_A = (X_i)_{i \in A}$, where $A \subseteq V$. For $A, B, C \subseteq V$, we say that X_A and X_B are conditional independent given X_C if the conditional density $f(\mathbf{x}_A | \mathbf{x}_B, \mathbf{x}_C)$ can be written as a function of \mathbf{x}_A and \mathbf{x}_C alone. This relation is usually denoted by $X_A \perp X_B | X_C$. Important properties of the conditional independence studied in Dawid (1979) are usually described as the *semi-graphoid axioms*. Let X, Y and Z be disjoint random variables, the graphoids axioms can be summarized as follows:

- If $X \perp Y | Z$ then $Y \perp X | Z$ (symmetry)
- If $X \perp Y | Z$ and U is a function of X , then $Y \perp U | Z$ (decomposition)
- If $X \perp Y | Z$ and U is a function of X , then $X \perp Y | (Z, U)$ (weak union)
- If $X \perp Y | Z$ and $X \perp W | (Y, Z)$ then $X \perp (W, Y) | Z$ (contraction)

It is standard to relate one semi-graphoid to another in terms of Markov properties, commonly that induced by the separation statements in a graph, see e.g. Paz and Pearl (1985).

Definition 4. *A distribution for X is said to be Markov with respect to G if for any decomposition (A, B) it holds that*

$$(5) \quad X_A \perp X_B | X_{A \cap B}.$$

For distributions which are Markov with respect to a graph G , the density follows the so-called *clique-separator-factorization* (CSF) property:

$$(6) \quad f(\mathbf{x}) = \frac{\prod_{Q \in \mathcal{Q}} f(\mathbf{x}_Q)}{\prod_{S \in \mathcal{S}} f(\mathbf{x}_S)}.$$

In the multivariate normal distribution, the underlying graph is determined by the precision matrix. We let the normal distributions with mean $\mathbf{m} \in \mathbb{R}^{|V|}$ and positive definite covariance $\Sigma \in \mathbb{R}^{|V| \times |V|}$ be denoted by $\mathcal{N}(\mathbf{m}, \Sigma)$. For a specific graph G , we denote by $\mathcal{N}_G(\mathbf{m}, \Sigma) = \{\mathcal{N}_G(\mathbf{m}, \Sigma) : \Sigma^{-1} \in \mathcal{P}_G\}$, where \mathcal{P}_G is the space of all symmetric positive definite matrices $\Sigma \in \mathbb{R}^{|V| \times |V|}$ such that $(\Sigma^{-1})_{ij} = 0$ whenever (i, j) is not an edge in G . This set of distributions is known as the Gaussian graphical model (GGM) or covariance selection model, and corresponds to those Gaussian distributions which are Markov with respect to G , see Dempster (1972); Speed and Kiiveri (1986).

Dawid and Lauritzen (1993) introduced an extension of the concept of Markov properties to distributions defined over distributions (referred to as *laws*). For parametric models where there is a one-to-one relationship between the parameter θ and the distribution, such distribution refers to a distribution over the parameter space. From a Bayesian perspective, when the distribution of X is completely determined by a random parameter θ , such laws are known as priors, denoted by $\mathcal{L}(\theta)$.

For $A, B \subseteq V$, the notation θ_A refers to the marginal distribution of X_A and $\theta_{A|B}$ determines the distribution of $(X_A | X_B = \mathbf{x}_B)$.

Definition 5. *A law $\mathcal{L}(\theta)$ is said to be (weak) hyper Markov with respect to G if for $A, B \subseteq V$*

$$\theta_A \perp \theta_B | \theta_{A \cap B}.$$

It is said to be strong hyper Markov if

$$\theta_A \perp \theta_{B|A}.$$

The strong hyper Markov property is of particular interest in Bayesian inference since it enables for posterior calculations to be performed locally using data collected separately for each clique, see (Dawid and Lauritzen, 1993, Corollary 5.5).

The following property is crucial in the construction of hyper Markov laws. For given two laws \mathcal{L}_A and \mathcal{L}_B , defined for θ_A and θ_B respectively where $A, B \subseteq V$, we say that \mathcal{L}_A and \mathcal{L}_B are *hyper consistent* if they both have the same marginal law on $\theta_{A \cap B}$. Given a set of hyper consistent laws $\{\mathcal{L}_Q : Q \in \mathcal{Q}\}$, the unique hyper Markov law is constructed by hyper combinations of the clique-specific laws.

3. GRAPHICAL PREDICTIVE CLASSIFICATION

We first restrict the attention to the single class case, implying that $n_c = n$ and focus attention on one clique $Q \in \mathcal{Q}$. In such setting, the data are assumed to be sampled from $\mathcal{N}(\mathbf{m}_Q, \Sigma_Q)$ and can be summarized by the joint density

$$(7) \quad f(\mathbf{x}_Q^{(n)} | \mathbf{m}_Q, \Sigma_Q) = (2\pi)^{-nq/2} |\Sigma_Q|^{-n/2} \exp \left\{ -\frac{1}{2} \sum_{i=1}^n (\mathbf{x}_Q^i - \bar{\mathbf{x}}_Q)' \Sigma_Q^{-1} (\mathbf{x}_Q^i - \bar{\mathbf{x}}_Q) \right\},$$

where $\bar{\mathbf{x}}_Q = \frac{1}{n} \sum_{i=1}^n \mathbf{x}_Q^i$. To simplify the notation, we temporarily drop the subscript by Q and let $q = q$. It is well known from Bayesian theory that the conjugate prior for (\mathbf{m}, Σ) is *normal inverse Wishart* which we denote by $\mathcal{NIW}(\boldsymbol{\mu}, \nu, \boldsymbol{\Phi}, \vartheta)$. In this distribution, the marginal of Σ is *inverse Wishart*, $\mathcal{IW}(\boldsymbol{\Phi}, \vartheta)$ with $\vartheta > q-1$ degrees of freedom and positive definite location matrix $\boldsymbol{\Phi}$. The conditional distribution of \mathbf{m} given Σ is $\mathcal{N}(\boldsymbol{\mu}, \frac{1}{\nu} \boldsymbol{\Sigma})$. The joint density is given by

$$(8) \quad \mathcal{NIW}(\mathbf{m}, \Sigma | \boldsymbol{\mu}, \nu, \boldsymbol{\Phi}, \vartheta) = \frac{1}{\kappa(\vartheta, \boldsymbol{\Phi}, \nu)} |\Sigma|^{-1/2} \exp \left\{ -\frac{\nu}{2} (\mathbf{m} - \boldsymbol{\mu})' \Sigma^{-1} (\mathbf{m} - \boldsymbol{\mu}) \right\} \times |\Sigma|^{-(\vartheta+q+1)/2} \exp \left\{ -\frac{1}{2} \text{tr}(\boldsymbol{\Phi} \Sigma^{-1}) \right\},$$

where

$$\kappa(\vartheta, \boldsymbol{\Phi}, \nu) = \frac{2^{\vartheta q/2} \Gamma_q(\vartheta/2)}{|\boldsymbol{\Phi}|^{\vartheta/2}} \frac{(2\pi)^{q/2}}{\nu^{\frac{1}{2}}}.$$

Γ_q is the multivariate gamma function defined as

$$\Gamma_q(a) = \pi^{q(q-1)/4} \prod_{i=0}^{q-1} \Gamma(a - \frac{i}{2}), \text{ for } a > (q-1)/2.$$

The posterior associated with $\mathbf{x}^{(n)}$ has the updated parameters

$$\nu^* = \nu + n, \boldsymbol{\mu}^* = \frac{\nu \boldsymbol{\mu} + n \bar{\mathbf{x}}}{\nu^*}, \vartheta^* = \vartheta + n \text{ and } \boldsymbol{\Phi}^* = \boldsymbol{\Phi} + \mathbf{S} + \frac{\nu n}{\nu^*} (\boldsymbol{\mu} - \bar{\mathbf{x}}) (\boldsymbol{\mu} - \bar{\mathbf{x}})',$$

where $\mathbf{S} = \sum_{i=1}^n (\mathbf{x}^i - \bar{\mathbf{x}})(\mathbf{x}^i - \bar{\mathbf{x}})'$. The posterior predictive distribution of \mathbf{x}^{n+1} , where the parameters are integrated out according to (2) is now written as

$$(9) \quad \int_{\mathcal{P}_{G_Q}} \int_{\mathbb{R}^q} \mathcal{N}(\mathbf{x}^{n+1} | \mathbf{m}, \boldsymbol{\Sigma}) \mathcal{N}IW(\mathbf{m}, \boldsymbol{\Sigma} | \boldsymbol{\mu}^*, \nu^*, \boldsymbol{\Phi}^*, \vartheta^*) d\mathbf{m} d\boldsymbol{\Sigma}.$$

This is the non-central multivariate t -distribution with density

$$\mathcal{T}(\mathbf{x}^{n+1} | \delta^*, \boldsymbol{\mu}^*, \boldsymbol{\Upsilon}^*) = \frac{\Gamma[(\delta^* + q)/2] |\boldsymbol{\Upsilon}^*|^{1/2}}{\Gamma(\delta^*/2) (\delta^* \pi)^{q/2}} \left[1 + (\boldsymbol{\mu}^* - \mathbf{x}^{n+1})' \boldsymbol{\Upsilon}^* (\boldsymbol{\mu}^* - \mathbf{x}^{n+1}) \right]^{-(\delta^* + q)/2},$$

where $\delta^* = \nu^* + 1 - q$ and $\boldsymbol{\Upsilon}^* = \frac{\nu^*(\nu^* + 1 - q)}{\nu^* + 1} \boldsymbol{\Phi}^{*-1}$, see e.g. (Bernardo and Smith, 2000, p. 441).

3.1. Hyper Markov laws over decomposable graphs. In the following we discuss how to obtain a predictive distribution of full dimension, p , that is not restricted to one specific clique. For this purpose, we first specify a joint prior law for $(\mathbf{m}, \boldsymbol{\Sigma})$, and show that it is strong hyper Markov with respect to G . Analogously to (9) the construction of the normal inverse Wishart law, we let the marginal law of $\boldsymbol{\Sigma}$ be the so called *hyper inverse Wishart law*, with $\vartheta > p - 1$ degrees of freedom and precision matrix $\boldsymbol{\Phi}$ satisfying

$$(10) \quad \sum_{Q \in \mathcal{Q}} [\boldsymbol{\Phi}_Q]^0 - \sum_{S \in \mathcal{S}} [\boldsymbol{\Phi}_S]^0 = \boldsymbol{\Phi},$$

where the notation $[A]^0$ is obtained from the matrix A by padding it with zeros to get the correct dimensions. This law was derived in Dawid and Lauritzen (1993) as the law obtained from hyper combinations of $\mathcal{IW}(\boldsymbol{\Phi}_Q, \vartheta)$ laws defined individually for each clique. Further, we specify the distribution of \mathbf{m} conditional on $\boldsymbol{\Sigma}$ as $\mathcal{N}(\boldsymbol{\mu}, \frac{1}{\nu} \boldsymbol{\Sigma})$, where $\boldsymbol{\mu} \in \mathbb{R}^p, \nu > 0$. We call the resulting law for the *hyper Normal inverse Wishart law* and denote it by $\mathcal{N}IW_G(\boldsymbol{\mu}, \nu, \boldsymbol{\Phi}, \vartheta)$. The density can be verified (see A.1) to follow the CSF property as

$$(11) \quad \mathcal{N}IW_G(\mathbf{m}, \boldsymbol{\Sigma} | \boldsymbol{\mu}, \nu, \boldsymbol{\Phi}, \vartheta) = \frac{\prod_{Q \in \mathcal{Q}} \mathcal{N}IW(\mathbf{m}_Q, \boldsymbol{\Sigma}_Q | \boldsymbol{\mu}_Q, \nu, \boldsymbol{\Phi}_Q, \vartheta)}{\prod_{S \in \mathcal{S}} \mathcal{N}IW(\mathbf{m}_S, \boldsymbol{\Sigma}_S | \boldsymbol{\mu}_S, \nu, \boldsymbol{\Phi}_S, \vartheta)}.$$

In order to show that the strong hyper Markov we restate Proposition 5.1 from Dawid and Lauritzen (1993).

Proposition 1. (Dawid and Lauritzen, 1993, Proposition 5.1) *If the prior law $\mathcal{L}(\theta)$ is hyper Markov over G then the joint distribution of (X, θ) satisfies, for any decomposition (A, B) of G ,*

$$(12) \quad (X_A, \theta_A) \perp (X_B, \theta_B) | (X_{A \cap B}, \theta_{A \cap B}).$$

If $\mathcal{L}(\theta)$ is strong hyper Markov, it also satisfies

$$(13) \quad (X_A, \theta_A) \perp (X_B, \theta_{B|A}) | X_{A \cap B}.$$

Proposition 2. *The hyper normal inverse Wishart law is strong hyper Markov.*

Proof. In light of (Dawid and Lauritzen, 1993, Proposition 5.1), where (X, θ) is substituted for (\mathbf{m}, Σ) , it follows from (12) that the distribution of (\mathbf{m}, Σ) is weak hyper Markov. The clique wise laws are the $\mathcal{N}\mathcal{IW}(\mu_Q, \nu, \Phi_Q, \vartheta)$ defines a full exponential family which are conjugate to the sampling distribution, thus by (Dawid and Lauritzen, 1993, Proposition 5.9), also the strong hyper Markov property holds for (\mathbf{m}, Σ) . \square

By (Dawid and Lauritzen, 1993, Corollary 5.2) the posterior is also strong hyper Markov and can be calculated using data corresponding to each clique. Further as stated in Dawid and Lauritzen (1993), by substituting X for X^{n+1} and θ for (\mathbf{m}, Σ) in Proposition 5.1, and letting $(\mathbf{m}, \Sigma) \sim \mathcal{N}\mathcal{IW}(\mu^*, \nu^*, \Phi^*, \vartheta^*)$, it follows from the weak union and the decomposition property of the semi-graphoid axioms (see Section 2) that the posterior predictive distribution for X^{n+1} is Markov. The clique-wise distributions are pairwise consistent $\mathcal{T}(\delta^*, \mu_Q^*, \Upsilon_Q^*)$ distributions, yielding the CSF property of the density

$$(14) \quad \mathcal{T}_G(\mathbf{x}^{n+1} | \delta^*, \mu_Q^*, \Upsilon_Q^*) = \frac{\prod_{Q \in \mathcal{Q}} \mathcal{T}(\mathbf{x}_Q^{n+1} | \delta^*, \mu_Q^*, \Upsilon_Q^*)}{\prod_{S \in \mathcal{S}} \mathcal{T}(\mathbf{x}_S^{n+1} | \delta^*, \mu_S^*, \Upsilon_S^*)}.$$

In the following this distribution will be referred to as the *non-central graph t-distribution* with δ^* degrees of freedom, mean vector μ^* and scale parameter $\Upsilon^* \in \mathcal{P}_G$.

3.2. Bayesian model averaging. In the above consideration, the graph is assumed to be fixed. In the present study, we take a BMA approach and incorporate uncertainty about the model by regarding G as a random variable, see e.g. Madigan et al. (1995). Byrne and Dawid (2015) introduced the family of structural Markov graph laws from which we choose the simplest, the uniform law defined as $p(G) = 1/|\mathcal{G}|$ for all $G \in \mathcal{G}$. The full hierarchical structure of data generation is then structured as follows

$$\begin{aligned} G &\sim \text{Unif}(\mathcal{G}) \\ \mathbf{m}, \Sigma \mid G &\sim \mathcal{N}\mathcal{IW}_G(\mu, \nu, \Phi, \vartheta) \\ X_i \mid \mathbf{m}, \Sigma &\sim \mathcal{N}_G(\mathbf{m}, \Sigma), \end{aligned}$$

for $i = 1, \dots, n+1$. In this setting, the predictive distribution in (2) also includes marginalizing over the space of decomposable graphs as

$$\sum_{G \in \mathcal{G}} \int_{\mathcal{P}_G} \int_{\mathbb{R}^p} f(\mathbf{x}^{n+1} | \mathbf{m}, \Sigma, G) f(\mathbf{m}, \Sigma, G | \mathbf{x}^{(n_c)}) d\mathbf{m} d\Sigma$$

which reduces (see A.2) to the following expression

$$(15) \quad f(\mathbf{x}^{n+1} | \mathbf{x}^{(n_c)}, c, \mathcal{C}^n) = \sum_{G \in \mathcal{G}} p(G | \mathbf{x}^{(n_c)}) \mathcal{T}_G(\mathbf{x}^{n+1} | \delta^*, \mu^*, \Upsilon^*),$$

where

$$(16) \quad p(G | \mathbf{x}^{(n_c)}) = \frac{f(\mathbf{x}^{(n_c)} | G) p(G)}{\sum_{G' \in \mathcal{G}} f(\mathbf{x}^{(n_c)} | G') p(G')}$$

is the graph posterior and

$$(17) \quad f(\mathbf{x}^{(n_c)} | G) = (2\pi)^{-np/2} \frac{\kappa_G(\vartheta^*, \Phi^*, \nu^*)}{\kappa_G(\vartheta, \Phi, \nu)}$$

is the marginal likelihood of G derived in A.3 where

$$\kappa_G(\vartheta, \Phi, \nu) = \frac{\prod_{Q \in \mathcal{Q}} \kappa_{G_Q}(\vartheta, \Phi_Q, \nu)}{\prod_{S \in \mathcal{S}} \kappa_{G_S}(\vartheta, \Phi_S, \nu)}$$

is the normalizing constant in $\mathcal{NIW}_G(\mathbf{m}, \Sigma | \boldsymbol{\mu}, \nu, \Phi, \vartheta)$.

The number of decomposable graphs with p nodes grows proportional to $\sum_r \binom{p}{r} 2^{r(p-r)}$, see Wormald (1985) and Rios et al. (2016) for exact enumeration and estimation of this quantity. Consequently exact computation of the marginalizing factor in (17) is intractable. We propose the particle Gibbs scheme with systematic refreshment introduced in Olsson et al. (2016) to give an approximation $\hat{p}(G|\mathbf{x}^{(n_c)})$ of $p(G|\mathbf{x}^{(n_c)})$, which is then plugged into (18) to give a predictive classifier in the sense of (3) explicitly written as

$$(18) \quad \sum_{G \in \mathcal{G}} \hat{p}(G|\mathbf{x}^{(n_c)}) \mathcal{T}_G(\mathbf{x}^{n+1} | \delta^*, \boldsymbol{\mu}^*, \boldsymbol{\Upsilon}^*).$$

4. PARTICLE GIBBS WITH SYSTEMATIC REFRESHMENT

In this section we describe the *particle Gibbs with systematic refreshment* (PG) sampling scheme established in Olsson et al. (2016), in the present context of approximating $p(G|\mathbf{x}^{(n_c)})$. The PG *sampler* constructs, using SMC, a Markov kernel \mathbf{P}_p^N leaving an extended version of the distribution $p(G|\mathbf{x}^{(n_c)})$, denoted by $\eta_{1:p}$ invariant. We proceed this section by defining $\eta_{1:p}$ by a procedure called *temporalization* and show its key property of having $p(G|\mathbf{x}^{(n_c)})$ as marginal distribution.

Step I. We first specify the target distribution of interest as the graph posterior, $p(G | \mathbf{x}^{(n_c)})$.

Step II. In this step of the temporalization we exploit the junction tree representation for decomposable graphs. Note that, having a distribution, $p(T)$ over the set of junction trees directly induces a distribution over the underlying decomposable graphs since

$$(19) \quad p(G) = \sum_{T: g(T)=G} p(T),$$

for any $G \in \mathcal{G}$. We use the junction tree posterior, introduced in Green and Thomas (2013) defined as

$$p(T | \mathbf{x}^{(n_c)}) = p(g(T) | \mathbf{x}^{(n_c)}) \times \frac{1}{\mu(g(T))} \propto p(\mathbf{x}^{(n_c)} | g(T)) \times \frac{1}{\mu(g(T))},$$

for any $T \in \mathcal{T}$. That is, each junction representation of any specific graph is assigned equal probability. With this definition, by combining the above equations, as shown in

Thomas and Green (2009) the induced graph distribution is the graph posterior of interest since

$$\sum_{T:g(T)=G} p(T \mid \mathbf{x}^{(n_c)}) = \sum_{T:g(T)=G} p(g(T) \mid \mathbf{x}^{(n_c)}) \times \frac{1}{\mu(g(T))} = p(G \mid \mathbf{x}^{(n_c)}).$$

Step III. In this step, we extend the junction tree representation and its distribution by a variable corresponding to the nodes in the underlying graph. Let, for all $m \in \{1, \dots, p\}$, Z_m be the space of all m -combinations of elements in $\{1, \dots, p\}$. An element $z_m \in Z_m$ is of form $z_m = (z_{1|m}, \dots, z_{m|m})$ where $\{z_{\ell|m}\}_{\ell=1}^m \subseteq \{1, \dots, p\}$ are distinct. For $(\ell, \ell') \in \{1, \dots, m\}^2$ such that $\ell \leq \ell'$, we denote $z_{\ell:\ell'|m} := (z_{\ell|m}, \dots, z_{\ell'|m})$. Denote by \mathcal{T}_{z_m} the space of junction trees with underlying graph nodes in $z_m \in Z_m$. We define, for all $m = 1, \dots, p$, the extended state spaces of junction trees with internal nodes in Z_m by

$$\mathcal{W}_m := \bigcup_{z_m \in Z_m} (\{z_m\} \times \mathcal{T}_{z_m}).$$

We define discrete probability distribution ψ_m on Z_m , for the extended target distributions

$$\eta_m(w_m) = \frac{\gamma_m(w_m)}{\sum_{w_m \in \mathcal{W}_m} \gamma_m(w_m)},$$

where

$$\gamma_m(w_m) := \psi_m(z_m) \times \frac{p(\mathbf{x}^{(n_c)} \mid g(T_{z_m}))}{\mu(g(T_{z_m}))}.$$

Moreover, since $Z_p = \{\{1, \dots, p\}\}$ we note that $\psi_p = \delta_{\{1, \dots, p\}}$, implying that $p(T_{z_p} \mid \mathbf{x}^{(n_c)})$ is the marginal distribution of η_p with respect to the T_{z_p} component. It is crucial that the distributions $\{\psi_m\}_{m=1}^p$ satisfies the recursion

$$\psi_{m+1}(z_{m+1}) = \sum_{z_m \in Z_m} \bar{\Psi}_m(z_m, z_{m+1}) \psi_m(z_m),$$

where

$$\bar{\Psi}_m(z_m, z_{m+1}) := \delta_{z_m}(z_{1:m|m+1}) \Psi_m(z_{1:m|m+1}, z_{m+1|m+1})$$

with Ψ_m being a Markov transition kernel density¹ from Z_m to $\{1, \dots, p\}$ such that $\Psi_m(z_m, j) = 0$ for all $j \in z_m$. Here we let for $j \in \{1, \dots, p\} \setminus z_m$,

$$\Psi_m(z_m, j) = \frac{1}{p-m},$$

where $m \geq 2$. Further, by letting

$$\psi_1(z_1) = \frac{1}{p},$$

we obtain at each step m , $\psi_m(z_m)$ as the uniform distribution over the nodes not in $\{1, \dots, p\} \setminus z_m$.

¹All densities on finite countable spaces in this paper are defined with respect to the counting measure on the same space.

Step IV. The last step in the temporalization is the extension to the path space $\mathcal{W}_{1:m} := \times_{\ell=1}^m \mathcal{W}_\ell$. On this space we define a proposal kernel \mathbf{K}_m of form

$$\mathbf{K}_m(w_m, w_{m+1}) = \bar{\Psi}_m(z_m, z_{m+1}) \mathbf{K}_m^* \langle z_m, z_{m+1} \rangle (T_m, T_{m+1}),$$

where $\bar{\Psi}_m$ is defined in (4) and for all $(z_m, z_{m+1}) \in \mathcal{Z}_m \times \mathcal{Z}_{m+1}$, $\mathbf{K}_m^* \langle z_m, z_{m+1} \rangle : \mathcal{T}_{z_m} \times \mathcal{T}_{z_{m+1}} \rightarrow [0, 1]$ is the so called Christmas tree kernel established in Rios et al. (2016).

The extension of γ_m to $\mathcal{W}_{1:m}$, is achieved through the backward versions of the kernels \mathbf{K}_m , denoted by $\mathbf{R}_m : \mathcal{W}_{m+1} \times \mathcal{W}_m \rightarrow [0, 1]$, where for each m ,

$$\mathbf{R}_m(w_{m+1}, w_m) := |\mathsf{S}_m(w_{m+1})|^{-1} \mathbb{1}_{\mathsf{S}_m(w_{m+1})}(w_m) \quad (w_{m+1} \in \mathcal{W}_{m+1}),$$

i.e., $\mathbf{R}_m(w_{m+1}, dw_m)$ is the uniform distribution over $\mathsf{S}_m(w_{m+1})$, the support of $\mathbf{K}_m(\cdot, w_{m+1})$. The resulting distribution on $\mathcal{W}_{1:m}$ is defined as

$$\bar{\gamma}_m(w_{1:m}) := \gamma_m(w_m) \prod_{\ell=1}^{m-1} \mathbf{R}_\ell(w_{\ell+1}, w_\ell).$$

Under this construction, since each \mathbf{R}_m is Markovian, the marginal distribution of w_p is exactly the distribution $p(T_{z_p} | \mathbf{x}^{(n_c)})$.

We use the notation $\Pr(\{a_\ell\}_{\ell=1}^N)$ to denote the categorical probability distribution induced by a set $\{a_\ell\}_{\ell=1}^N$ of positive (possibly unnormalised) numbers; thus, writing $W \sim \Pr(\{a_\ell\}_{\ell=1}^N)$ means that the variable W takes the value $\ell \in \{1, \dots, N\}$ with probability $a_\ell / \sum_{\ell'=1}^N a_{\ell'}$.

The algorithm is as follows. It is initiated by one draw, $W_{1:p}^1 \sim \Pr(\{\omega_p^\ell\}_{\ell=1}^N)$, where the weights $\{\omega_p^\ell\}_{\ell=1}^N$ are generated by the standard SMC algorithm stated in Algorithm 1. Then the PG kernel is applied to generate samples $W_{1:p}^2, W_{1:p}^3, \dots$. Algorithmically, the more or less only difference between the PG kernel and the standard SMC algorithm is that the PG kernel, which is described in detail in Algorithm 2, evolves the particle cloud *conditionally* on a fixed reference trajectory specified *a priori*; this *conditional SMC* algorithm is constituted by Lines 1–16 in Algorithm 2. After having evolved, for p time steps, the particles of the conditional SMC algorithm, the PG kernel draws randomly a particle from the last generation (Lines 17–19). It then samples a new genealogical history of the selected particle back to the first generation using the backward kernel (Lines 20–22), and returns the traced path (Line 23). The backward sampling procedure is the so called refreshment step which serves to improve mixing. For a complete presentation of the PG sampler and related results see Olsson et al. (2016) and Andrieu et al. (2010).

It can be shown that \mathbf{P}_p^N is $\eta_{1:p}$ -reversible and thus leaves $\eta_{1:p}$ invariant, see (Chopin and Singh, 2015, Proposition 8). Thus, on the basis of \mathbf{P}_p^N , the PG sampler generates (after possible burn-in) a Markov chain $\{W_{1:p}^\ell\}_{\ell=1}^M$ according to

$$W_{1:p}^1 \xrightarrow{\mathbf{P}_p^N} W_{1:p}^2 \xrightarrow{\mathbf{P}_p^N} W_{1:p}^3 \xrightarrow{\mathbf{P}_p^N} \dots \xrightarrow{\mathbf{P}_p^N} W_{1:p}^M,$$

where $W_{1:p}^l \in \mathcal{W}_p$, $l = 1, \dots, M$. An unbiased estimator of $p(T \mid \mathbf{x}^{(n_c)})$ is obtained as

$$\hat{p}(T \mid \mathbf{x}^{(n_c)}) = \frac{1}{M} \sum_{\ell=1}^M \mathbb{1}_T(T_p^\ell),$$

where each T_p^ℓ variable is extracted, on Line 18, at iteration $\ell - 1$ of Algorithm 2. The estimator of $p(G \mid \mathbf{x}^{(n_c)})$ now follows directly as $\hat{p}(G \mid \mathbf{x}^{(n_c)}) = \sum_{T: g(T)=G} \hat{p}(T \mid \mathbf{x}^{(n_c)})$.

Data: $\{(\xi_m^i, \omega_m^i)\}_{i=1}^N$
Result: $\{(\xi_{m+1}^i, \omega_{m+1}^i)\}_{i=1}^N$

1 **for** $i \leftarrow 1, \dots, N$ **do**

2 draw $I_{m+1}^i \sim \Pr(\{\omega_m^\ell\}_{\ell=1}^N)$;

3 draw $z_{m+1}^i \sim \Psi_m(z_m^{I_{m+1}^i}, dz_{m+1})$;

4 draw $T_{m+1}^i \sim \mathbf{K}_m^* \langle z_m^{I_{m+1}^i}, z_{m+1}^i \rangle (T_m^{I_{m+1}^i}, dT_{m+1})$;

5 set $\xi_{m+1}^i \leftarrow (z_{m+1}^i, T_{m+1}^i)$;

6 set $\omega_{m+1}^i \leftarrow \frac{p(\mathbf{x}^{(n_c)} \mid g(T_{z_{m+1}}^i)) \mu(g(T_{z_m}^{I_{m+1}^i})) \mathbf{R}_m(\xi_m^{I_{m+1}^i}, \xi_{m+1}^i)}{p(\mathbf{x}^{(n_c)} \mid g(T_{z_m}^{I_{m+1}^i})) \mu(g(T_{z_{m+1}}^i)) \mathbf{K}_m^* \langle z_m^{I_{m+1}^i}, z_{m+1}^i \rangle (T_m^{I_{m+1}^i}, T_{m+1}^i)}$;

Algorithm 1: SMC update.

Data: a reference trajectory $w_{1:p} \in \mathcal{W}_{1:p}$
Result: a draw $W_{1:p}$ from $\mathbf{P}_p^N(w_{1:p}, \cdot)$

```

1 for  $i \leftarrow 1, \dots, N-1$  do
2   draw  $z_1^i \sim \psi_1(z_1)$  ;
3   set  $T_1^i \leftarrow (\{z_1^i\}, \emptyset)$  ;
4   set  $\xi_1^i \leftarrow (z_1^i, T_1^i)$  ;
5   set  $\xi_1^N \leftarrow w_1$  ;
6   for  $i \leftarrow 1, \dots, N$  do
7     set  $\omega_1^i \leftarrow 1$  ;
8   for  $m \leftarrow 1, \dots, p-1$  do
9     for  $i \leftarrow 1, \dots, N-1$  do
10    draw  $I_{m+1}^i \sim \Pr(\{\omega_m^\ell\}_{\ell=1}^N)$  ;
11    draw  $z_{m+1}^i \sim \bar{\Psi}_m(z_m^{I_m^i}, \cdot)$  ;
12    draw  $T_{m+1}^i \sim \mathbf{K}_m^*(z_m^{I_m^i}, z_{m+1}^i)(T_m^{I_m^i}, \cdot)$  ;
13    set  $\xi_{m+1}^i \leftarrow (z_{m+1}^i, T_{m+1}^i)$  ;
14   set  $\xi_{m+1}^N \leftarrow w_{m+1}$  ;
15   for  $i \leftarrow 1, \dots, N$  do
16     set  $\omega_{m+1}^i \leftarrow \frac{p(\mathbf{x}^{(n_c)} | g(T_{z_{m+1}}^i)) \mu(g(T_{z_m}^{I_m^i})) \mathbf{R}_m(\xi_m^{I_m^i}, \xi_{m+1}^i)}{p(\mathbf{x}^{(n_c)} | g(T_{z_m}^{I_m^i})) \mu(g(T_{z_{m+1}}^i)) \mathbf{K}_m^*(z_m^{I_m^i}, z_{m+1}^i)(T_m^{I_m^i}, T_{m+1}^i)}$  ;
17   draw  $J_p \sim \Pr(\{\omega_p^\ell\}_{\ell=1}^N)$  ;
18   set  $T_p \leftarrow T_p^{J_p}$  ;
19   set  $W_p \leftarrow (\{1, \dots, p\}, T_p)$  ;
20   for  $m \leftarrow p-1, \dots, 1$  do
21     draw  $W_m \sim \mathbf{R}_m(W_{m+1}, \cdot)$  ;
22   set  $W_{1:p} \leftarrow (W_1, \dots, W_p)$  ;
23 return  $W_{1:p}$ 

```

Algorithm 2: One transition of PG.

5. NUMERICAL STUDY

We demonstrate the performances of the suggested BMA classifier by one realistic- and four synthetic datasets, illustrating different typical classification scenarios. In each of the examples the underlying graph distribution was estimated by the PG sampler, where the number of particles, N were set to 50 and the number of Gibbs samples, M where set to 2000. The burn-in period where deduced by visual inspection of likelihood traces of the sampled graphs. The CT proposal kernels $\{\mathbf{K}_m\}_{m=1}^p$ of the SMC algorithm has two tuning parameters, α and β which were both set to 0.5, reflecting an assumption of moderately

sparse graphs. We refer to Rios et al. (2016) for a more detailed description of how of these parameters influence the sparsity of the generated junction trees.

The performance of our classifier were compared to 11 different out-of-the-box classifiers. We also included the BMA classifier where the graph distributions was set to be a point mass at the true graph respectively. For further details about the implementation and parameterization of these classifiers, the reader is referred to the python library for this paper available at https://bitbucket.org/flrios/graphical_predictive_classifier.

5.1. Synthetic data. The number of nodes in each of the synthetic examples were fixed to $p = 50$ and the graphs were generated by the CTA with $\alpha = 0.5$ and $\beta = 0.5$. For each example and each class c , the data were sampled from $\mathcal{N}_{G_c}(\mathbf{m}_c, \boldsymbol{\Sigma}_c)$, where the subscript c now indicates class belonging. We defined $\boldsymbol{\Sigma}_c$ so as to fulfill

$$(\boldsymbol{\Sigma}_c)_{ij} = \begin{cases} \sigma^2, & \text{if } i = j \\ \rho\sigma^2, & \text{if } (i, j) \in G_c \end{cases}$$

and $(\boldsymbol{\Sigma}_c^{-1})_{ij} = 0$ if $(i, j) \notin G_c$. This is the graphical intraclass structure considered in Thomas and Green (2009). Here, we have fixed the variance and correlation parameters σ^2 and ρ to 1.0 and 0.5 respectively. The underlying graph and class centroids, \mathbf{m}_c for the three scenarios are described below.

A) Two classes with different graphs. The class centroids where separated as $\mathbf{m}_1 = \mathbf{0}$ and $\mathbf{m}_2 = \Delta \times \mathbf{1}$, where $\mathbf{0}$ and $\mathbf{1}$ are the vectors of zeros and ones respectively and $\Delta = 0.0001$.

B) Three classes with different graphs. The class centroids in this example where separated as $\mathbf{m}_1 = \mathbf{0}$, $\mathbf{m}_2 = ((i \bmod 2) \times \Delta)_{i=1}^p$ and $\mathbf{m}_3 = ((i + 1 \bmod 2) \times \Delta)_{i=1}^p$ and $\Delta = 0.0001$.

These choices of separating the class centroids showed to reflect narrowness between the classes. For each of the scenarios, the correct classification rate was calculated on 10 independently generated datasets each consisting of 50 test samples for each class. The training datasets consisted of $n = 51$ and $n = 300$ samples for each class. The correct classification probability was then estimated by their mean and summarized in Table 1.

The hyper parameters for the hyper normal inverse Wishart prior were set to $\nu = 1$, $\boldsymbol{\Phi} = \mathbf{I}$ and $\vartheta = p$ in all classes for each of the examples. For $\boldsymbol{\mu}_c$ we used the empirical mean computed separately in each of the classes.

The results of the graph posterior estimation by the PG sampler for one of the 10 dataset replicates from example A and B shown in Figure 1-3. The first row in each figure show the adjacency matrices for the underlying graphs in each of the classes and the second row shows the estimated heatmaps. A dark color at position i, j , counted from the top left corner, indicates high marginal posterior probability of the edge (i, j) . It is interesting note that even though the pattern in the heatmaps fro the $n = 51$ case does not resemble those in the the corresponding underlying graph so well, the BMA classifier still performs better than the standard Bayesian predictive classifier as seen in Table 1. Also, with this small amount of data one could hardly expect to see the true pattern in the posterior heatmaps. For $n = 300$, we observe better correspondence between the heatmap and the true underlying graph, and the true classification probability is also higher. However, the

	Walking	A, $n = 300$	A, $n = 51$	B, $n = 51$
Bayes pred	0.809 (0.050)	0.888 (0.041)	0.725 (0.040)	0.613 (0.052)
BMA (true)	-	0.948 (0.015)	0.904 (0.037)	0.877 (0.029)
BMA (PG)	0.848 (0.059)	0.933 (0.025)	0.816 (0.047)	0.788 (0.038)
3-NN	0.825 (0.053)	0.716 (0.054)	0.670 (0.040)	0.558 (0.026)
Gauss proc	0.829 (0.046)	0.700 (0.047)	0.652 (0.029)	0.538 (0.028)
Dec tree (5)	0.761 (0.045)	0.548 (0.050)	0.543 (0.063)	0.373 (0.047)
Naive Bayes	0.740 (0.071)	0.480 (0.026)	0.504 (0.042)	0.340 (0.036)
Linear SVM	0.644 (0.070)	0.471 (0.041)	0.487 (0.032)	0.358 (0.050)
Neural net	0.774 (0.098)	0.825 (0.047)	0.631 (0.050)	0.521 (0.036)
AdaBoost	0.791 (0.051)	0.488 (0.053)	0.496 (0.036)	0.331 (0.036)
LDA	0.666 (0.044)	0.482 (0.031)	0.490 (0.038)	0.348 (0.047)
QDA	0.741 (0.095)	0.889 (0.041)	0.535 (0.032)	0.391 (0.022)
Rand forest	0.700 (0.078)	0.541 (0.055)	0.526 (0.057)	0.348 (0.040)

TABLE 1. Estimated probabilities (standard errors) of correct classification averaged over the 10 test sets for the walking / Nordic walking data and the synthetic datasets.

impact of the graph seem to degrease when the number of data increases, since the standard Bayesian predictive classifier shows comparable results toe to our BMA approach, (0.89 to 0.93). For the $n = 51$ case, there is a greater gap between the standard approach and the BMA approach (0.73 to 0.82).

The third row shows the log-likelihood for the sampled graphs (blue line), the true underlying graph (green line) and the complete graph (red line), where the complete graph corresponds to the standard Bayesian posterior predictive classifier. As the log-likelihood for the complete graph is substantially lower than those sampled by the PG sampler for both classes, the plot illustrates the motivation of the BMA approach. Remarkably, the log-likelihood for the true underlying graph is also lower than those samples by the PG sampler in the $n = 51$ case. This is explained by the relatively small amount of data that we are using, for $n = 300$ the plots has the expected relation.

The last row shows the estimated auto-correlations of the number of edges in the graphs (*graph size*) generated by the PG sampler. The dependence seem to decline to zero after about 100-200 lags. Both the autocorrelation and the heatmaps were estimated after a burn-in period, deduced from the log-likelihood plots.

Throughout each of the examples, the BMA classifier showed better results than the standard Bayesian predictive approach using the similar parametrization. Also the BMA classifier out performed the rest of the classifiers as well. The BMA classifier with point mass at the true graph is the best choice in each of the examples.

5.2. Realistic data: walking and Nordic walking. This dataset was first introduced in Reiss and Stricker (2012a,b) where eighteen different physical activities were measured

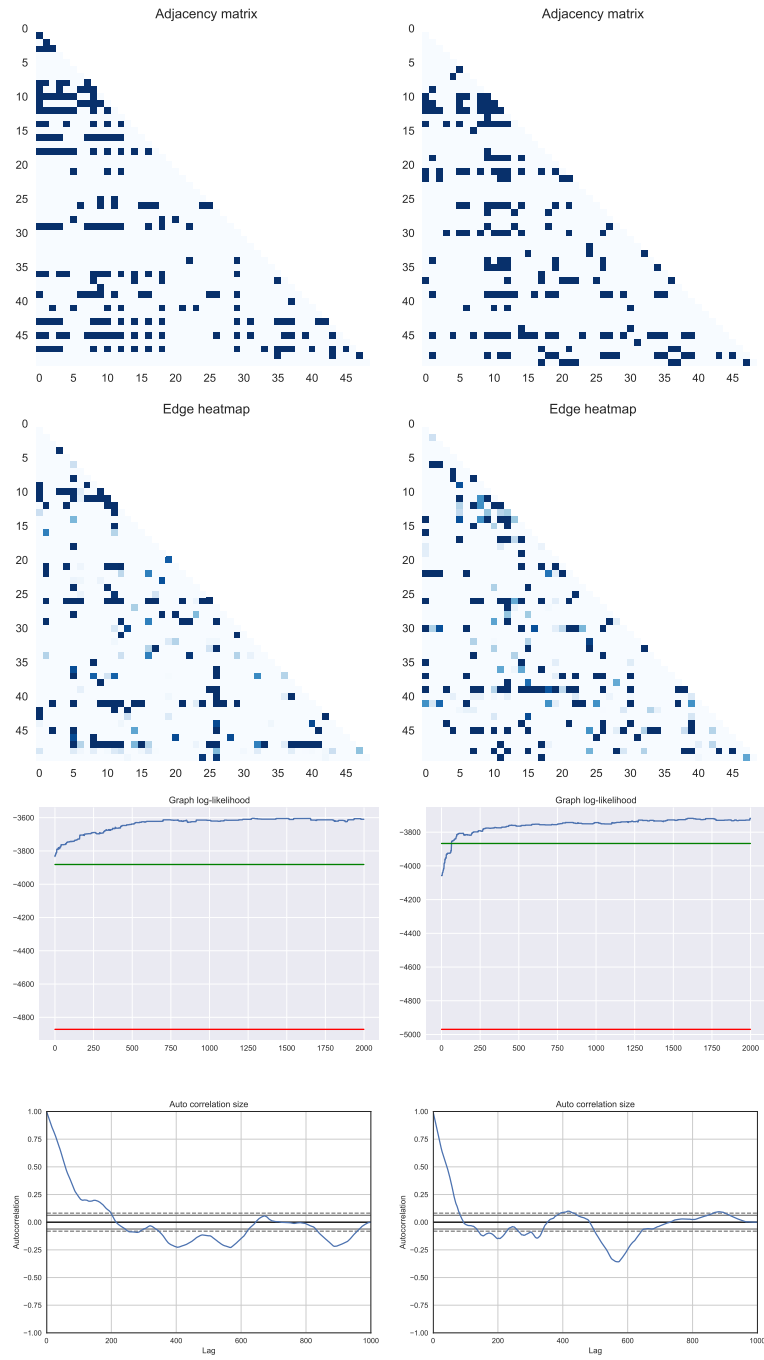
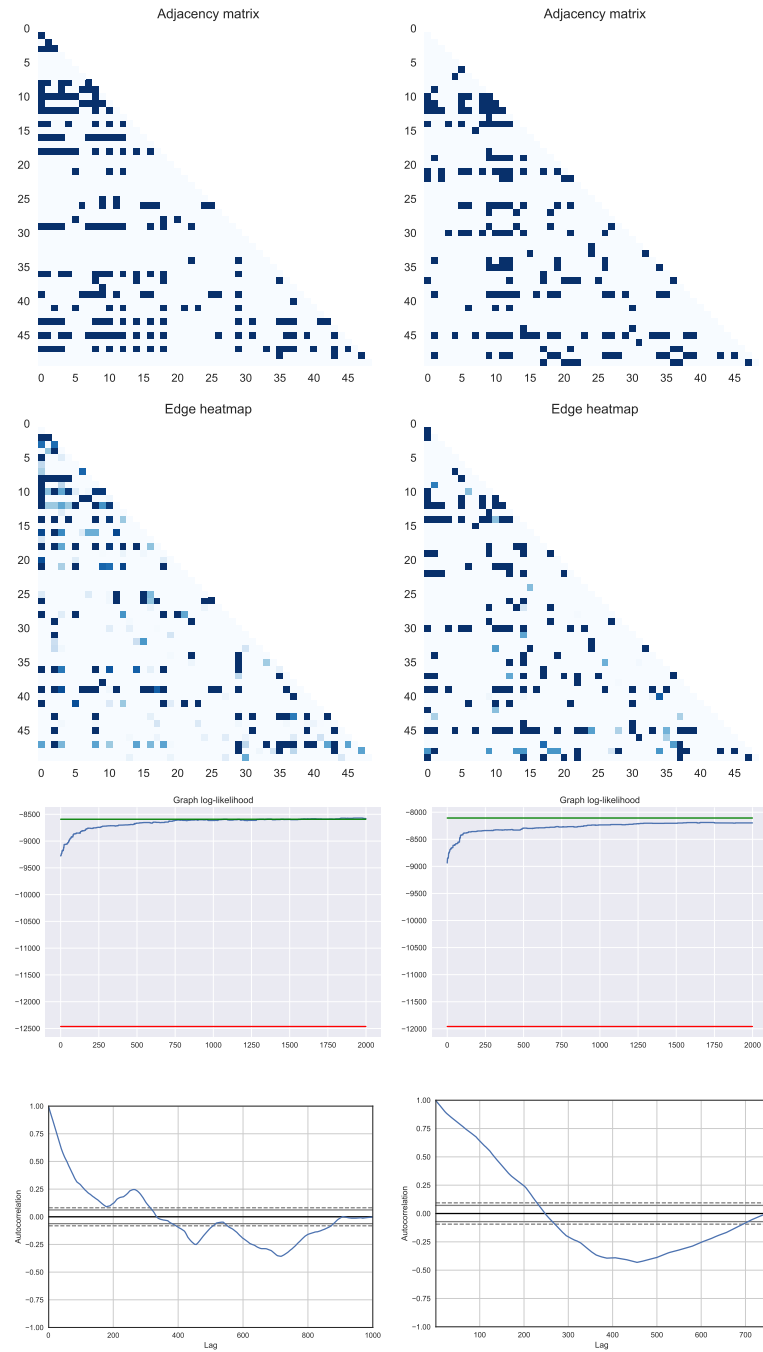


FIGURE 1. Dataset A.

FIGURE 2. Dataset A, $n = 300$.

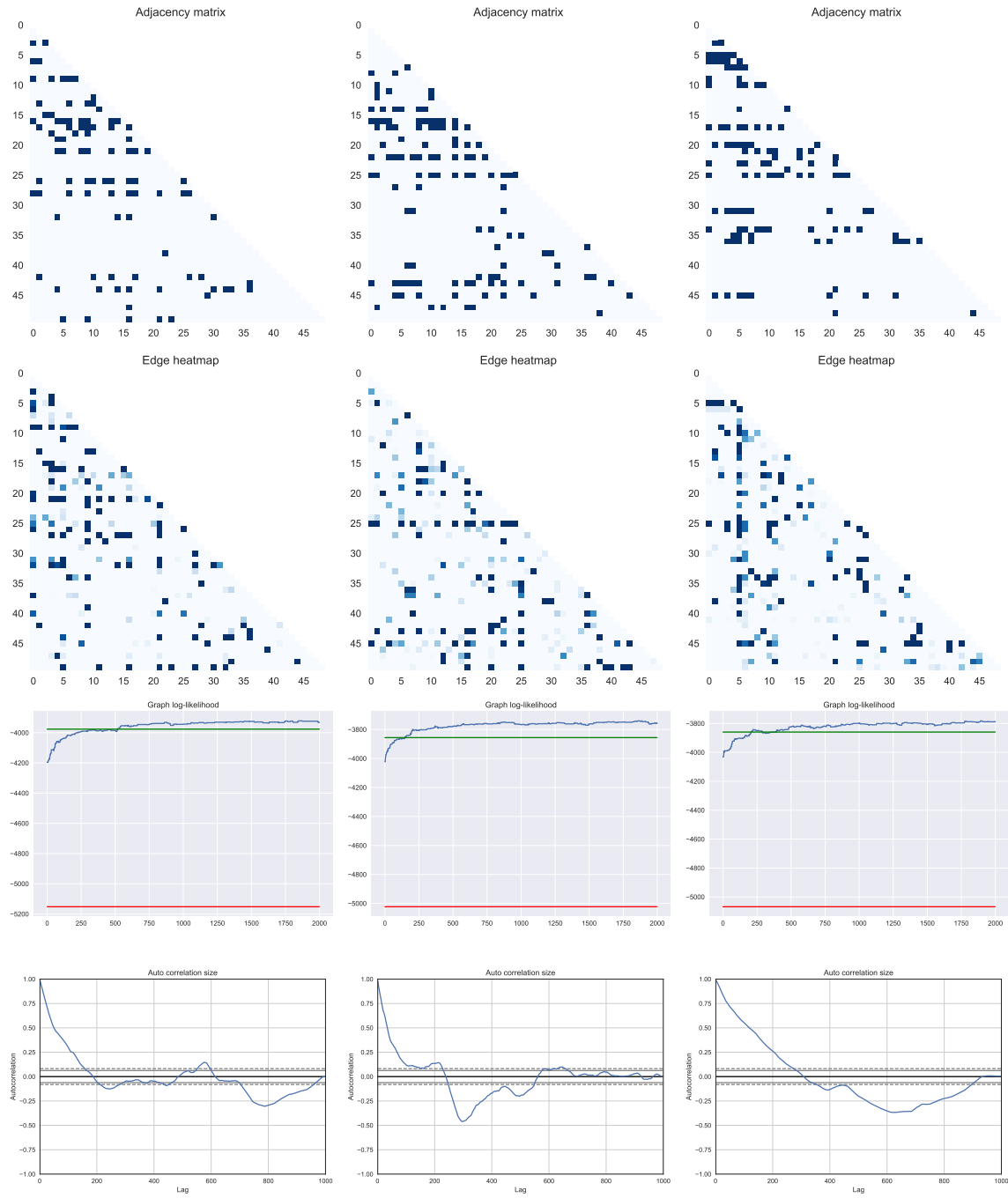


FIGURE 3. Dataset B.

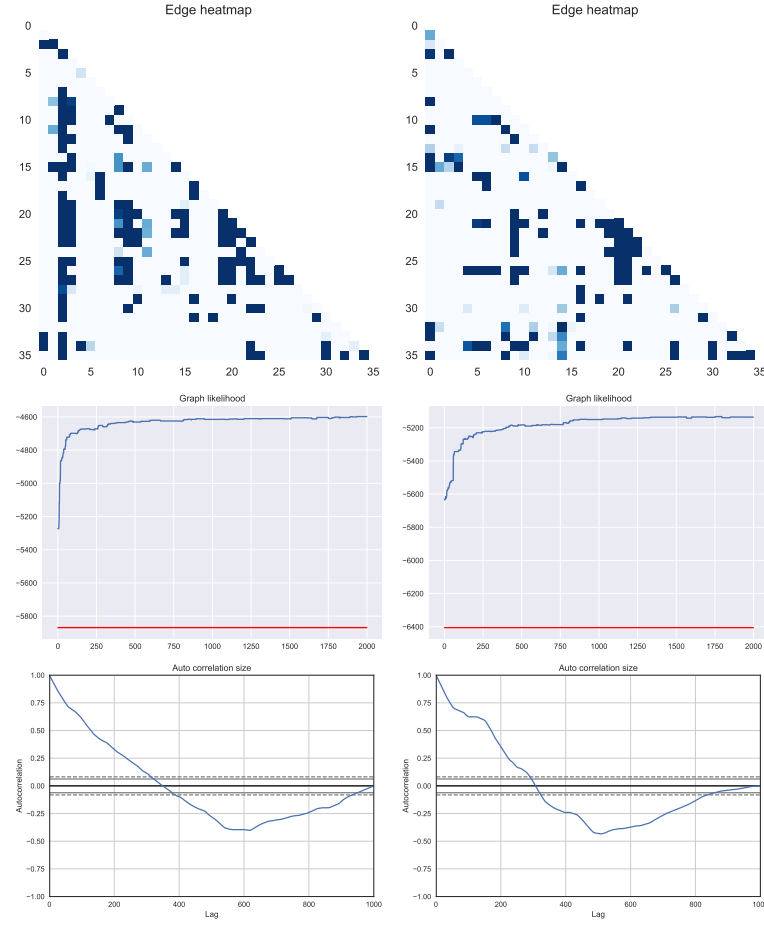


FIGURE 4. Walking/Nordic walking.

on eight subjects. The data was collected at a rate of 100Hz using three wireless IMUs (inertial measurement units) placed on strategic location at the body; one IMU over the wrist on the dominant arm, one IMU on the chest and one IMU on the dominant side's ankle. The measurements were then summarized in 52-dimensional vectors. However, some of these measurements were categorical and thus dropped here yielding a reduction in dimension to $p = 36$. For this study, we selected the subject referred to as *Subject1* and study the two types of activities, *walking* to *Nordic walking* thereby determining a two-class classification problem. Walking was performed outside with a speed of 4-6km/h, according to what was suitable for the subject. Nordic walking was performed on asphaltic terrain, using asphalt pads on the walking poles.

In total the full dataset contains ≈ 12000 data vectors, which enabled us to generate classification data with a similar strategy as in the synthetic data by sampling without replacement 10 replicates of 50 test and $n = 40$ training samples from the full dataset for each

class. Consequently, we ignore the possible time dependence between the samples which we could expect. We set the hyper parameters ν, Φ, ϑ and μ_c analogously to the synthetic data examples above. The results from the PG sampler for the two classes are found in Figure 4. For the log-likelihood plots, we deduce that the PG sampler seem to have reach a stationary distributions after about 1000 iterations. The results of correct classification are found in Table 1. We see that also in this realistic scenario where the underlying graph structure is unknown, our suggested particle Gibbs BMA classifier outperforms the standard predictive classifier as well as the out-of-the-box classifiers.

6. CONCLUSION

We have constructed a theoretical framework for Bayesian predictive classification where the model uncertainty is taken into account, by regarding the graph structure underlying the data as random and by using the BMA approach. Specifically, at the averaging step of the BMA, each predictive posterior for a fresh \mathbf{x}^{n+1} was weighted by the graph posterior $p(G_c | \mathbf{x}^{(n_c)})$.

Computing $p(G_c | \mathbf{x}^{(n_c)})$, except for toy problems, remains a hard task even for moderate p . Our solution to this problem was to use an approximation obtained by the particle Gibbs sampler suggested in Olsson et al. (2016).

As a part of the graph posterior specification, we have derived the hyper normal inverse Wishart law and showed that it has the strong hyper Markov property. We also showed that the posterior predictive distribution for \mathbf{x}^{n+1} , obtained by marginalising out the parameters following the hyper normal inverse Wishart law, has the non-central graph t -distribution and concluded that this distribution is Markov.

The results of the numerical study demonstrated that the particle Gibbs BMA approach to predictive classification indeed improved performance accuracy of the standard Bayesian predictive classifier (corresponding to a point mass at the complete graph) for four synthetic datasets as well as for the realistic walking/Nordic walking dataset, where the true underlying graph structure was unknown.

A comparison with 11 standard out-of-the-box classifiers was also performed, showing that our suggested BMA predictive classifier has systematically superior performance.

Though promising results of the suggested methodology were obtained, a deeper theoretical analysis of the computational complexity along with further numerical validation is needed; for example other more flexible graph priors for both the graph and the parameters are interesting subjects for further study, which is of special importance for applications in high-dimensional problems.

APPENDIX A.

A.1. Derivation of (11). Since $\Sigma \sim \mathcal{IW}_G(\Phi, \vartheta)$, it holds that $\sum_{Q \in \mathcal{Q}} [\Sigma_Q]^0 - \sum_{S \in \mathcal{S}} [\Sigma_S]^0 = \Sigma$, which implies that both the determinant and the trace in decomposes in the expression

below (see e.g. Lauritzen (1996))

$$\begin{aligned}
\mathcal{N}(\mathbf{m}|\boldsymbol{\mu}, \frac{1}{\nu}\boldsymbol{\Sigma})\mathcal{IW}_G(\boldsymbol{\Sigma}|\boldsymbol{\Phi}, \vartheta) &= (2\pi)^{-\frac{p}{2}}|\frac{1}{\nu}\boldsymbol{\Sigma}|^{-1/2} \exp\left\{-\frac{\nu}{2} \text{tr}((\mathbf{m} - \boldsymbol{\mu})(\mathbf{m} - \boldsymbol{\mu})' \boldsymbol{\Sigma}^{-1})\right\} \times \mathcal{IW}_G(\boldsymbol{\Sigma} \mid \boldsymbol{\Phi}, \vartheta) \\
&= \frac{\prod_{Q \in \mathcal{Q}} \mathcal{N}(\mathbf{m}_Q|\boldsymbol{\mu}_Q, \frac{1}{\nu}\boldsymbol{\Sigma}_Q)}{\prod_{S \in \mathcal{S}} \mathcal{N}(\mathbf{m}_S|\boldsymbol{\mu}_S, \frac{1}{\nu}\boldsymbol{\Sigma}_S)} \times \frac{\prod_{Q \in \mathcal{Q}} \mathcal{IW}(\boldsymbol{\Sigma}_Q \mid \boldsymbol{\Phi}_Q, \vartheta)}{\prod_{S \in \mathcal{S}} \mathcal{IW}(\boldsymbol{\Sigma}_S \mid \boldsymbol{\Phi}_S, \vartheta)} \\
&= \frac{\prod_{Q \in \mathcal{Q}} \mathcal{N}\mathcal{IW}(\mathbf{m}_Q, \boldsymbol{\Sigma}_Q \mid \boldsymbol{\mu}_Q, \nu, \boldsymbol{\Phi}_Q, \vartheta)}{\prod_{S \in \mathcal{S}} \mathcal{N}\mathcal{IW}(\mathbf{m}_S, \boldsymbol{\Sigma}_S \mid \boldsymbol{\mu}_S, \nu, \boldsymbol{\Phi}_S, \vartheta)} \\
&= \mathcal{N}\mathcal{IW}_G(\mathbf{m}, \boldsymbol{\Sigma} \mid \boldsymbol{\mu}, \nu, \boldsymbol{\Phi}, \vartheta).
\end{aligned}$$

A.2. Derivation of (18). (Dawid and Lauritzen, 1993, p. 1296) showed that the predictive distribution for strong hyper Markov laws are Markov so that

$$\begin{aligned}
f(\mathbf{x}^{n+1} \mid \mathbf{x}^{(n_c)}, c, \mathcal{C}^n, G) &= \int_{\mathcal{P}_G} \int_{\mathbb{R}^p} f(\mathbf{x}^{n+1} \mid \mathbf{m}, \boldsymbol{\Sigma}) f(\mathbf{m}, \boldsymbol{\Sigma} \mid G, \mathbf{x}^{(n_c)}) d\mathbf{m} d\boldsymbol{\Sigma} \\
&= \int_{\mathcal{P}_G} \int_{\mathbb{R}^p} \mathcal{N}(\mathbf{x}^{n+1} \mid \mathbf{m}, \boldsymbol{\Sigma}) \mathcal{N}\mathcal{IW}_G(\mathbf{m}, \boldsymbol{\Sigma} \mid \boldsymbol{\mu}^*, \nu^*, \boldsymbol{\Phi}^*, \vartheta^*) d\mathbf{m} d\boldsymbol{\Sigma} \\
&= \frac{\prod_{Q \in \mathcal{Q}} \int_{\mathcal{P}_G} \int_{\mathbb{R}^p} \mathcal{N}(\mathbf{x}^{n+1} \mid \mathbf{m}_Q, \boldsymbol{\Sigma}_Q) \mathcal{N}\mathcal{IW}(\mathbf{m}_Q, \boldsymbol{\Sigma}_Q \mid \boldsymbol{\mu}_Q^*, \nu^*, \boldsymbol{\Phi}_Q^*, \vartheta^*) d\mathbf{m}_Q d\boldsymbol{\Sigma}_Q}{\prod_{S \in \mathcal{S}} \int_{\mathcal{P}_G} \int_{\mathbb{R}^p} \mathcal{N}(\mathbf{x}^{n+1} \mid \mathbf{m}_S, \boldsymbol{\Sigma}_S) \mathcal{N}\mathcal{IW}(\mathbf{m}_S, \boldsymbol{\Sigma}_S \mid \boldsymbol{\mu}_S^*, \nu^*, \boldsymbol{\Phi}_S^*, \vartheta^*) d\mathbf{m}_S d\boldsymbol{\Sigma}_S} \\
&= \mathcal{T}_G(\mathbf{x}^{n+1} \mid \boldsymbol{\delta}^*, \boldsymbol{\mu}^*, \boldsymbol{\Upsilon}^*),
\end{aligned}$$

thus we can write

$$\begin{aligned}
f(\mathbf{x}^{n+1} \mid \mathbf{x}^{(n_c)}, c, \mathcal{C}^n) &= \sum_{G \in \mathcal{G}} \int_{\mathcal{P}_G} \int_{\mathbb{R}^p} f(\mathbf{x}^{n+1} \mid \mathbf{m}, \boldsymbol{\Sigma}, G) f(\mathbf{m}, \boldsymbol{\Sigma}, G \mid \mathbf{x}^{(n_c)}) d\mathbf{m} d\boldsymbol{\Sigma} \\
&= \sum_{G \in \mathcal{G}} \int_{\mathcal{P}_G} \int_{\mathbb{R}^p} f(\mathbf{x}^{n+1} \mid \mathbf{m}, \boldsymbol{\Sigma}, G) f(\mathbf{m}, \boldsymbol{\Sigma} \mid G, \mathbf{x}^{(n_c)}) f(G \mid \mathbf{x}^{(n_c)}) d\mathbf{m} d\boldsymbol{\Sigma} \\
&= \sum_{G \in \mathcal{G}} p(G \mid \mathbf{x}^{(n_c)}) \int_{\mathcal{P}_G} \int_{\mathbb{R}^p} f(\mathbf{x}^{n+1} \mid \mathbf{m}, \boldsymbol{\Sigma}) f(\mathbf{m}, \boldsymbol{\Sigma} \mid G, \mathbf{x}^{(n_c)}) d\mathbf{m} d\boldsymbol{\Sigma} \\
&= \sum_{G \in \mathcal{G}} p(G \mid \mathbf{x}^{(n_c)}) f(\mathbf{x}^{n+1} \mid \mathbf{x}^{(n_c)}, c, \mathcal{C}^n, G) \\
&= \sum_{G \in \mathcal{G}} p(G \mid \mathbf{x}^{(n_c)}) \mathcal{T}_G(\mathbf{x}^{n+1} \mid \boldsymbol{\delta}^*, \boldsymbol{\mu}^*, \boldsymbol{\Upsilon}^*).
\end{aligned}$$

A.3. Derivation of (17). We super script a density by * to denote its unnormalized version. Since the hyper inverse Wishart is a conjugate prior for the normal model, we

have

$$\begin{aligned}
f(\mathbf{x}^{(n_c)}|G) &= \int_{\mathcal{P}_G} \int_{\mathbb{R}^p} \mathcal{N}(\mathbf{x}^{(n_c)}|\mathbf{m}, \boldsymbol{\Sigma}) \mathcal{N} \mathcal{IW}_G(\mathbf{m}, \boldsymbol{\Sigma}|\boldsymbol{\mu}, \nu, \boldsymbol{\Phi}, \vartheta) d\mathbf{m} d\boldsymbol{\Sigma} \\
&= (2\pi)^{-np/2} \frac{1}{\kappa_G(\vartheta, \boldsymbol{\Phi}, \nu)} \int_{\mathcal{P}_G} \int_{\mathbb{R}^p} \mathcal{N}^*(\mathbf{x}^{(n_c)}|\mathbf{m}, \boldsymbol{\Sigma}) \mathcal{N} \mathcal{IW}_G^*(\mathbf{m}, \boldsymbol{\Sigma}|\boldsymbol{\mu}, \nu, \boldsymbol{\Phi}, \vartheta) d\mathbf{m} d\boldsymbol{\Sigma} \\
&= (2\pi)^{-np/2} \frac{1}{\kappa_G(\vartheta, \boldsymbol{\Phi}, \nu)} \int_{\mathcal{P}_G} \int_{\mathbb{R}^p} \mathcal{N} \mathcal{IW}_G^*(\mathbf{m}, \boldsymbol{\Sigma}|\boldsymbol{\mu}^*, \nu^*, \boldsymbol{\Phi}^*, \vartheta^*) d\mathbf{m} d\boldsymbol{\Sigma} \\
&= (2\pi)^{-np/2} \frac{\kappa_G(\vartheta^*, \boldsymbol{\Phi}^*, \nu^*)}{\kappa_G(\vartheta, \boldsymbol{\Phi}, \nu)}.
\end{aligned}$$

REFERENCES

C. Andrieu, A. Doucet, and R. Holenstein. Particle Markov chain Monte Carlo methods. *Journal of the Royal Statistical Society: Series B (Statistical Methodology)*, 72(3):269–342, 2010.

J. Bernardo and A. Smith. *Bayesian Theory*. Wiley, Chichester, 2000.

S. Byrne and A. P. Dawid. Structural Markov graph laws for Bayesian model uncertainty. *Annals of Statistics*, 43(4):1647–1681, 2015.

N. Chopin and S. S. Singh. On particle Gibbs sampling. *Bernoulli*, 21(3):1855–1883, 08 2015.

M. Clyde and E. I. George. Model uncertainty. *Statistical science*, pages 81–94, 2004.

J. Corander, Y. Cui, and T. Koski. Inductive inference and partition exchangeability in classification. In *Algorithmic Probability and Friends. Bayesian Prediction and Artificial Intelligence*, pages 91–105. Springer, 2013a.

J. Corander, Y. Cui, T. Koski, and J. Sirén. Have I seen you before? Principles of Bayesian predictive classification revisited. *Statistics and Computing*, 23(1):59–73, Jan 2013b.

J. Corander, T. Koski, T. Pavlenko, and A. Tillander. *Bayesian block-diagonal predictive classifier for Gaussian data*, pages 543–551. Springer Berlin Heidelberg, Berlin, Heidelberg, 2013c.

Y. Cui, J. Sirén, T. Koski, and J. Corander. Simultaneous predictive gaussian classifiers. *Journal of Classification*, 33(1):73–102, Apr 2016.

A. Dawid and B. Fang. Conjugate Bayes discrimination with infinitely many variables. *Journal of multivariate analysis*, 41(1):27–42, 1992.

A. P. Dawid. Conditional independence in statistical theory. *Journal of the Royal Statistical Society. Series B (Methodological)*, 41(1):1–31, 1979.

A. P. Dawid and S. L. Lauritzen. Hyper Markov laws in the statistical analysis of decomposable graphical models. *The Annals of Statistics*, 21(3):1272–1317, 09 1993.

A. P. Dempster. Covariance selection. *Biometrics*, 28(1):pp. 157–175, 1972.

S. Geisser. Posterior odds for multivariate normal classifications. *Journal of the Royal Statistical Society. Series B (Methodological)*, pages 69–76, 1964.

S. Geisser. Predictive discrimination. *Krishnajah, P.R. ed. Multivariate analysis*, 149:163, 1966.

S. Geisser. *Predictive inference: An introduction*. Chapman & Hall, London, 1993.

P. J. Green and A. Thomas. Sampling decomposable graphs using a Markov chain on junction trees. *Biometrika*, 100(1):91–110, 2013.

R. E. Kass and A. E. Raftery. Bayes factors. *Journal of the american statistical association*, 90(430):773–795, 1995.

S. L. Lauritzen. *Graphical Models*. Oxford University Press, 1996.

D. Madigan and A. E. Raftery. Model selection and accounting for model uncertainty in graphical models using Occam’s window. *Journal of the American Statistical Association*, 89(428):1535–1546, 1994.

D. Madigan, J. York, and D. Allard. Bayesian graphical models for discrete data. *International Statistical Review / Revue Internationale de Statistique*, 63(2):215–232, 1995.

H. Nyman, J. Xiong, J. Pensar, and J. Corander. Marginal and simultaneous predictive classification using stratified graphical models. *Advances in Data Analysis and Classification*, 10(3):305–326, 2016.

J. Olsson, T. Pavlenko, and F. L. Rios. Particle MCMC methods or non-temporal distribution flows with application to Bayesian structure learning in decomposable graphical models. 2016.

A. Paz and J. Pearl. *Graphoids: A graph based logic for reasoning about relevance relations*. UCLA, 1985.

A. Reiss and D. Stricker. Creating and benchmarking a new dataset for physical activity monitoring. In *Proceedings of the 5th International Conference on Pervasive Technologies Related to Assistive Environments*, page 40. ACM, 2012a.

A. Reiss and D. Stricker. Introducing a new benchmarked dataset for activity monitoring. In *Wearable Computers (ISWC), 2012 16th International Symposium on Wearable Computers*, pages 108–109. IEEE, 2012b.

F. L. Rios, J. Olsson, and T. Pavlenko. A Markovian kernel for generating junction trees of decomposable graphs. 2016.

B. D. Ripley. *Pattern recognition and neural networks*. Cambridge university press, 2007.

T. P. Speed and H. T. Kiiveri. Gaussian Markov distributions over finite graphs. *The Annals of Statistics*, 14(1):138–150, 1986.

A. Thomas and P. J. Green. Enumerating the junction trees of a decomposable graph. *Journal of Computational and Graphical Statistics*, 18(4):930–940, 2009.

N. C. Wormald. Counting labelled chordal graphs. *Graphs and Combinatorics*, 1(1):193–200, 1985.